Study on Deformation and Subsidence Measurement of Prefractured Sandstone under Dynamic Loading

Xin Wang, Shiliang Wu*

College of Energy and Mining Engineering, Shandong University of Science and Technology, Qingdao 266590, China

* Corresponding author: wangxinzuiniule@163.com

Abstract. The measurement of deformation and settlement of the ground surface under the action of dynamic loads is one of the urgent problems faced by geotechnical engineering. The rock mass is a non-homogeneous material and there are often a large number of non-penetrating fractures within the matrix. The rock mass deformation characteristics are directly influenced by these cracks, thereby accelerating the subsidence of the rock mass surface. The surface of the fractured rock mass is often subjected to dynamic impacts such as earthquakes, resulting in subsidence and deformation. The present study utilizes Hopkinson pressure bars and focuses on sandstone as the primary research subject. Prefabricated cracks are set at 0°, 30°, 60°, and 90° angles to measure and investigate the deformation and settlement behavior of specimens under dynamic impacts. The measurement results indicate that the increase of the prefabricated fracture angle gradually deteriorated the overall dynamic compressive performance of the sandstone, and the maximum stress of the sandstone specimen containing prefabricated fracture occurred at the prefabricated fracture angle of 0°, with the maximum average dynamic peak stress of 62.39 MPa. This study extends the researchers understanding of the deformation and sedimentation characteristics of precast crushed sandstone under dynamic influence.

Keywords: rock deformation; Settlement measurement; SHPB; prefabricated fractures; dynamic stress

1 INTRODUCTION

The nature of the rock body determines the stability of rock engineering [1]. Especially under the condition that resource exploitation is gradually moving towards deeply buried rock layers, the rock body often contains joints and fractures, and these unstable factors increase the risk of underground engineering [2-3]. At the same time, underground engineering in its service life, not only to withstand the static pressure of the ground stress, but also often subject to mechanical excavation, blasting, rock explosion, and microseismic and other kinds of engineering and natural dynamic disturbances [4-6]. This puts higher requirements on the construction of underground engineering. Therefore, the study of the dynamic impact behavior of prefabricated rock

Q. Gao et al. (eds.), *Proceedings of the 2024 7th International Conference on Structural Engineering and Industrial Architecture (ICSEIA 2024)*, Atlantis Highlights in Engineering 30,
https://doi.org/10.2991/978-94-6463-429-7_11

masses is of great significance for the measurement of overlying rock deformation and surface subsidence.

The current research on rock bodies containing fractures mainly focuses on the mechanical characteristics of the objects under static loading. Li[7] conducted uniaxial compression tests on coal bodies with prefabricated fractures at different angles and found that the prefabricated crack angle had a significant effect on the mechanical properties of the coal samples, and the peak stresses and peak strains increased with the increase of the prefabricated crack angle, and the relationship with the prefabricated crack angle satisfied the quadratic function relationship. Chen[8] studied the type I crack expansion law of prefabricated cracks, through a device that simulates the directional expansion of rock cracks, and found that for different prefabricated lengths of cracks, their initial crack angles were mainly affected by the length of the cracks, and increasing the length of the prefabricated cracks was favorable to the expansion of the cracks at their tips. At the end of crack expansion, with the increase of prefabricated crack angle, Li[9-10] found that the stress concentration location at the crack tip began to spread outward from the center of the specimen, and the damage mode changed from tensile-shear composite mode to tensile-crack damage mode. In addition to uniaxial compression tests, Duan[11-12] used four semicircular loess specimens with different angles of prefabricated cracks for three-point bending tests, which showed that the fracture damage of the specimens was essentially a process of new cracks appearing at the tips of the prefabricated cracks and developing along a certain trajectory upward to the loading point. Further, Gong[13-14] conducted a series of loading and unloading tests on granite containing prefabricated fissures under high circumferential pressure conditions, which indicated that the cracks propagated in an intermittent or stepwise manner, and that the increase in the brittleness index under the unloading path of high circumferential pressure reflected a more pronounced brittle damage characteristic. The study on the rock mass containing prefabricated cracks showed that the smaller the angle between the loading direction and the angle of the prefabricated cracks, the higher the pressure the rock mass can withstand, which is a stable law in the study of static mechanics.

Although there have been many studies on rock dynamics, little research has been done on deformation and subsidence measurement of prefabricated fractured rock masses under dynamic mechanical effects. Whether prefabricated fractured rocks under dynamic impacts are consistent with static conditions remains to be further explored. Therefore, the deformation and subsidence of prefabricated fractured sandstone specimens at different angles under dynamic impacts were measured using Hopkinson pressure bars to obtain their mechanical characteristics.

2 METHODS

In order to fit the actual condition of the site as much as possible, the sandstone obtained from the in-situ coring of the coal mine was used, which was cut and polished to become a standard specimen with a diameter of 50mm and a height of 50mm. The specimen was processed by wire-cutting machine with the midpoint of the specimen axis as the center. The prefabricated fracture had a length of 20 mm and a width of 3 mm, with an overall capsule shape. The angle of the prefabricated fracture cut along the axial direction of the specimen was 0, and the prefabricated fracture was cut sequentially at 30 degrees and 60 degrees and 90 degrees totaling four different angles. The preparation process of the specimen is shown in Figure 1.

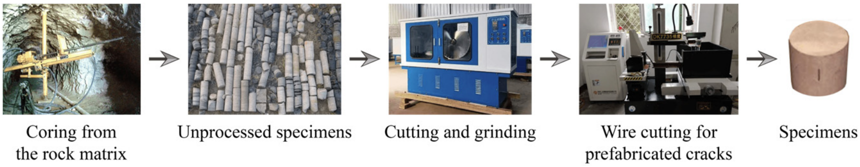

Fig. 1. Process for prefabricated sand stone specimens

The test equipment used a split Hopkinson pressure bar, which mainly included an impact device (firing barrel and bullet), a compression bar device (incident bar, transmission bar, absorption bar, and buffer device), and a signal acquisition device (laser, ultra-dynamic signal acquisition and processing device), as shown in Figure 2a. The impact of the bullet on the free end of the incident bar would generate an incident wave, and when the stress wave traveled to the contact interface between the end of the incident bar and the specimen, due to the difference in wave impedance, a part of the incident wave was reflected as a reflective wave, and the rest passes through the specimen to reach the transmission bar, forming a transmitted wave, as shown in Figure 2b. In addition, the velocity of the bullet was directly measured by a simple optical method, and the strain signal was collected by a Wheatstone bridge circuit with amplification.

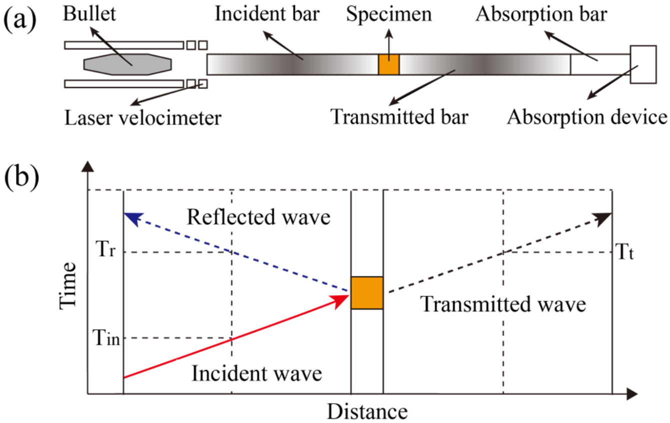

Fig. 2. (a) Sketch of SHPB. (b) Wave propagation of SHPB.

Prior to testing, molybdenum disulfide was applied to both ends of each specimen to reduce the effect of "end friction effect" on the stresses in the specimen.Each sample is hit once before testing, mainly to check the speed of the bullet. On the other hand, it also enables the stress waves inside the rod to propagate uniformly. At this point, when the incident wave and reflected wave are almost identical in the time integration region, and the transmitted wave region approaches 0, it indicates that the stress balance in the system can be carried out in subsequent tests.At the same time,four different prefabricated fracture angles (0°, 30°, 60°and 90°) and three different impact velocities (6m/s, 8m/s and 10m/s) were set up for orthogonal tests. Each group was repeated three times to ensure the accuracy of the results. The specific test parameters are shown in Table 1.

Table 1. Impact velocity of specimens (m/s)

Sample	Prefabricated cracks angle			
	0°	30°	60°	90°
6-1	6.75	5.75	5.54	6.55
6-2	5.90	6.22	6.22	5.08
6-3	6.64	6.48	6.99	6.49
8-1	7.30	7.06	7.87	7.51
8-2	8.58	8.72	7.36	8.34
8-3	7.77	7.45	8.67	7.54
10-1	10.58	9.50	9.04	10.11
10-2	9.06	9.79	10.05	9.17
10-3	9.86	10.84	9.84	9.81

3 RESULTS

The SHPB test is based on the one-dimensional stress wave assumption and the stress uniformity assumption: the one-dimensional stress wave assumption assumes that the stress wave in the compression bar is a one-dimensional elastic wave, and that the stresses in the specimen and the bar are one-dimensional; the stress uniformity assumption assumes that the stresses are uniform everywhere in the specimen in the specimen loading direction. Therefore, the strain rate , strain εs and stress σs of the specimen are calculated according to the following equations:

$$\dot{\varepsilon}_s = \frac{C_0}{l_s}\left[\varepsilon_i(t) - \varepsilon_r(t) - \varepsilon_t(t)\right] \tag{1}$$

and

$$\varepsilon_s = \frac{C_0}{l_s}\int_0^{t_0}\left[\varepsilon_i(t) - \varepsilon_r(t) - \varepsilon_t(t)\right]\mathrm{d}t \tag{2}$$

and

$$\sigma_s = \frac{EA}{2A_s}\left[\varepsilon_i(t) - \varepsilon_r(t) - \varepsilon_t(t)\right] \tag{3}$$

The stresses and strains of the specimens with different prefabricated fracture angles at different impact velocities were calculated according to Equations 1 to 3 and the maximum stresses were recorded as shown in Table 2. The measurement and calculation results are shown in Figure 4.

Table 2. Measurement results of peak stress of the sample

Sample	Prefabricated cracks angle			
	0°	30°	60°	90°
6-1	46.40	42.21	33.02	30.89
6-2	44.38	40.38	30.84	28.19
6-3	42.12	39.56	29.61	28.49
8-1	53.22	49.89	43.28	40.60
8-2	52.91	46.87	39.78	39.77
8-3	50.47	45.44	38.37	37.48
10-1	65.51	59.52	51.87	45.30
10-2	61.38	57.38	49.11	44.32
10-3	60.28	56.64	48.86	44.46

With the increase of prefabricated fracture angle, the peak stress of the specimen decreased continuously. Taking the impact velocity of 6 m as an example, when the prefabricated fracture angle of the specimen was 0°, the peak stress of the specimen was 42.12-46.40 MPa, with an average of 44.30 MPa. When the prefabricated fracture angle was increased to 30°, the peak stress of the specimen was 39.56-42.21 MPa, with an average of 40.72 MPa, compared with that of the prefabricated fracture of 0°, the peak stress of the specimen has decreased. When the prefabricated fracture angle was increased to 90°, the peak stress of the specimen reached the minimum, and the peak stress of the specimen ranges from 28.49 to 30.89 MPa, with an average of 29.19 MPa. It can be seen from the relationship between the prefabricated fracture angle and the peak stress that the increase of the prefabricated fracture angle deteriorated the overall impact resistance of the specimen. When the prefabricated fracture was in the same direction as the loading direction of the stress wave, the impact received by the specimen will bring more damage to the specimen.

With the increase of impact velocity, the peak stress of the specimen increased. The angle of the prefabricated fracture was 60° as an example, when the impact velocity of the specimen was 6m/s, the peak stress of the specimen was 29.61~33.02 MPa, with an average of 31.16MPa. When the impact velocity was increased to 8 m/s, the peak stress of the specimen was 38.37~43.28 MPa, with an average of 40.48 MPa, which was compared to that of the impact velocity of 6 m/s, the peak stress of the specimen was improved. When the impact velocity was increased to 10 m/s, the peak stress of the specimen reached the maximum, and the peak stress of the specimen was 48.86~51.87 MPa, with an average of 49.95 MPa. It is a general rule that the peak stress increases with the increase of the impact velocity in the SHPB system.

The stress-strain curves of homogeneous sandstone specimens containing prefabricated fracture under different impact velocities were clearly distinguished in each stage. One typical specimen each with different impact velocities and different prefabricated fracture angles was selected, and their stress and strain curves were plotted as shown in Figure 3. When the impact velocity was 6 m/s, none of the specimens with four prefabricated fracture angles (0°, 30°, 60°, 90°) showed macroscopic damage. At the beginning of the impact loading section, the distinction between their stress-strain curves was not obvious, and the climb rate of stress was basically the same. However, as the impact was loaded, more and more energy was accumulated on the specimens, and the specimens at 60° and 90° were more unable to withstand the energy carried by the stress wave compared with the specimens at 0° and 30°, which showed lower peak stresses. The specimens at 0° and 30° were able to carry larger strains, which peaked after the stress continued to climb for a period of time. The four groups of specimens with different prefabricated fracture angles all showed rebound stress-strain curves after the peak, i.e., "closed-mouth" curves, which was a typical sign that the specimens were not damaged. When the impact velocity was 8 m/s, the stress-strain curves of the specimens with four prefabricated fracture angles (0°, 30°, 60°, 90°) were more obviously differentiated. The four groups of specimens basically reached the peak stress in the same strain range, but the peak stress-strain curves of the specimens with 0° prefabricated fracture had higher slopes in the preloading section, which indicated that the prefabricated fracture at this angle could assist the specimens to deform, thus obtaining better impact resistance. When the impact velocity reached 10 m/s, each specimen reached their relative maximum peak stress. The stress-strain curves of the four groups of specimens with different prefabricated fracture angles were more distinguishable compared to the impact velocities of 6m/s and 8m/s. A prefabricated fracture angle of 90° possessed the lowest strain range, while specimens with a prefabricated fracture angle of 0° had the largest strain range. It was found by measuring the deformation and settlement characteristics of the specimens that regardless of the external impact velocity, the peak stress of the specimen is always the highest when the pre-cut fracture angle is 0, indicating that the specimen with a fracture angle of 0 has the best impact resistance.

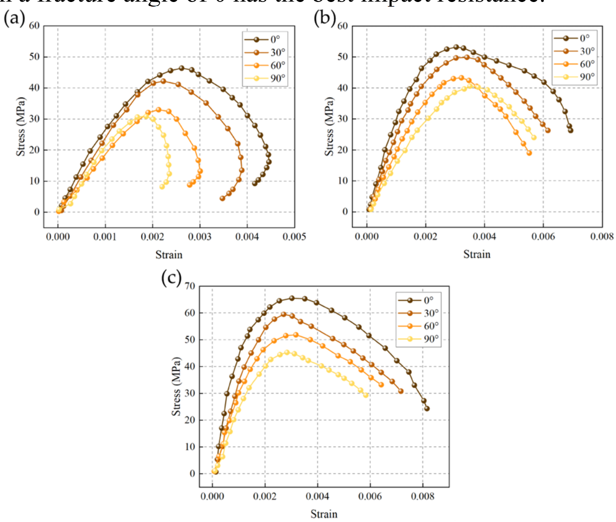

Fig. 3. Typical stress-strain curves of specimens: (a) 6m/s, (b) 8m/s, and (c) 10m/s.

After measurement, it was found that the peak stresses of the specimens with different prefabricated fracture angles showed a good linear relationship with the impact velocity. The average values of the peak stresses of the specimens with different cleavage angles were linearly fitted to the impact velocity, plotted as shown in Figure 4b, and the parameters of the linear fit are shown in Table 3. It can be seen that in general the peak stress of the specimen was decreasing as the prefabricated fracture angle increased. The slope of the linear fit was -0.1830 with an intercept of 44.58 when the impact velocity was 6 m/s. When the impact velocity was 8 m/s, the slope of the linear fit was -0.1552 with an intercept of 51.90. When the impact velocity was 10 m/s, the slope of the linear fit was -0.2033 with an intercept of 62.87. The three sets of linear fits had a high level of confidence, which were all above 0.90 or above. This indicates that 0° was still the optimal angle for impact resistance in the case of homogeneous sandstone containing cracks at a certain angle.

Table 3. Linear fit of each parameter of stress to prefabricated cracks angle.

Sample	Slope	Intercept	R^2
6m/s	-0.1830	44.58	0.9079
8m/s	-0.1552	51.90	0.9134
10m/s	-0.2033	62.87	0.9846

Note: R2 denotes the goodness of fitting.

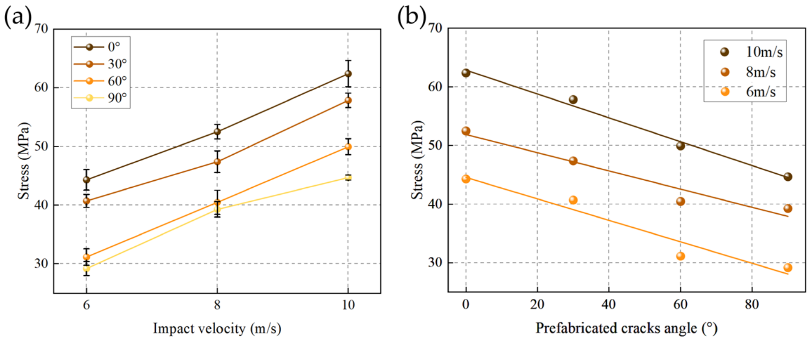

Fig. 4. (a) Average stress of specimens with different impact velocity. (b) Linear fitting of stress to prefabricated cracks angle.

4 CONCLUSION

The deformation and subsidence characteristics of sandstone with pre-existing cracks at different angles under dynamic impact were measured using the Hopkinson pressure bar dynamic impact test system in this study. The research focuses on the deformation and subsidence engineering of sandstone with pre-existing cracks under dynamic conditions. The overall dynamic compressive performance of the sandstone has been progressively deteriorated, and its mechanical properties have been reduced, making it more susceptible to settlement, as revealed by the measurements conducted. The maximum stress of the sandstone specimens containing prefabricated fracture occurred when the prefabricated fracture angle was 0, and the maximum average dynamic peak stress was 62.39 MPa (impact velocity was 10 m/s). The minimum stress occurred when the prefabricated fracture angle was 90, and the minimum average dynamic peak stress was 44.69 MPa (impact velocity was 10 m/s). The study will contribute to the enrichment of the engineering of deformation and settlement of fractured rock masses affected by dynamic loads.

Reference

1. Mao H. Y., Xu N. W., Zhou Z., Sha C., Xiao P. W. and Li B., "Failure mechanism and deformation forecasting of surrounding rock mass in an underground cavern based on engineering analogy method," Tunnelling and Underground Space Technology, Papers 143, 105497(2024).
2. Du W. X., Qian C. X. and Xie Y. D., "Demonstration application of microbial self-healing concrete in sidewall of underground engineering: A case study," Journal of Building Engineering, Papers 63, 105512(2023).
3. Wang H., Huai H. Y., Xu Z. C., Shang S. C., Zhou H. and Xing X. Y., "Study on mechanical properties of new supporting materials for soft rock underground engineering," Construction and Building Materials, Papers 408, 133631(2023).
4. He M. M., Ding M. C., Yuan Z. Y., Zhao J. R., Luo B. and Ma X. D., "Numerical simulation of rock bursts triggered by blasting disturbance for deep-buried tunnels in jointed rock masses," Computers and Geotechnics, Papers 161, 105609(2023).
5. Pan Y. S. and Wang A. W., "Disturbance response instability theory of rock bursts in coal mines and its application," Geohazard Mechanics, Papers 1, 1-17(2022).
6. Wang R. , Chen S. J., Li X. L., Tian G. and Zhao T. B., "AdaBoost-driven multi-parameter real-time warning of rock burst risk in coal mines," Engineering Applications of Artificial Intelligence, Papers 125, 106591(2023).
7. Li Z. H., Tian H., Niu Y., Wang E. Y., Zhang X., He S., Wang F.Z. and Zheng A. Q., "Study on the acoustic and thermal response characteristics of coal samples with various prefabricated crack angles during loaded failure under uniaxial compression," Journal of Applied Geophysics, Papers 200, 104618(2022).
8. Chen L. X., Guo W. Y., Zhang D. X. and Zhao T. B., "Experimental study on the influence of prefabricated fissure size on the directional propagation law of rock type-I crack," International Journal of Rock Mechanics and Mining Sciences, Papers 160, 105274(2022).
9. Li B., He Y. Z., Li L., Zhang J. X., Shi Z. and Zhang Y. P., "Damage evolution of rock containing prefabricated cracks based on infrared radiation and energy dissipation," Theoretical and Applied Fracture Mechanics, Papers 125, 103853(2023).
10. Lee O S, Kim M S. Dynamic material property characterization by using split Hopkinson pressure bar (SHPB) technique[J]. Nuclear Engineering and Design, 2003, 226(2): 119-125.
11. Duan Z., Dong C. X., Yan X. S., Sun Q. and Li B. , "Experimental research of fracture damage behavior of loess with different prefabricated cracks," Engineering Fracture Mechanics, Papers 275, 108849 (2022).
12. Larbi G, Mostapha T, Hocine O, et al. A practical note for SHPB test with new algorithms for delimiting pulses[J]. Composite Structures, 2015, 126: 145-158.
13. Gong H. L., Luo Y. , Xu K. , Huang J. H., Wang G. and Li X. P., "Failure behaviors of fractured granite during loading and unloading under high confining pressure based on acoustic emission multi-parameter analysis," Theoretical and Applied Fracture Mechanics, Papers 121, 103442(2022).
14. Jankowiak T, Rusinek A, Voyiadjis G Z. Modeling and design of SHPB to characterize brittle materials under compression for high strain rates[J]. Materials, 2020, 13(9): 2191.